CONDENSED MATTER PHYSICS

PHASE TRANSITIONS OF CESIUM NITRATE EMBEDDED IN NANOPOROUS ALUMINA FILMS

A.V. Pavlov[1], *E.V. Stukova*[1✉], *S.V. Baryshnikov*[2]

[1] Amur State University, Blagoveshchensk, Russia

[2] Blagoveshchensk State Pedagogical University, Blagoveshchensk, Russia

✉ lenast@bk.ru

Abstract. In order to make material with improved properties, nanocomposites based on nanoporous Al_2O_3 films (having different pore sizes) filled with ferroelectric, namely, cesium nitrate $CsNO_3$, have been fabricated, and their electrophysical charactistics have been investigated. The film surfaces were tested by electron microscopy. Temperature dependences of the effective permittivity ε' and of the third harmonic coefficient were measured for the nanocomposites. The phase-transition points were determined by the maximum value of the $d\varepsilon'/dT$ derivative. The reduction in pore was found to lead to a decrease in the Curie temperature (by more than 30 K) and a phase transition blur. This phenomenon is associated with the influence of intrinsic size effects.

Keywords: ferroelectric, cesium nitrate, permittivity, phase transition, nanocomposite

ФАЗОВЫЕ ПЕРЕХОДЫ НИТРАТА ЦЕЗИЯ, ВНЕДРЕННОГО В НАНОПОРИСТЫЕ ПЛЕНКИ ОКСИДА АЛЮМИНИЯ

А. В. Павлов[1], *Е. В. Стукова*[1✉], *С. В. Барышников*[2]

[1] Амурский государственный университет, г. Благовещенск, Россия;

[2] Благовещенский государственный педагогический университет, г. Благовещенск, Россия

✉ lenast@bk.ru

Аннотация. С целью создания материала с улучшенными сегнетоэлектрическими свойствами были изготовлены нанокомпозиты на основе нанопористых пленок Al_2O_3 (с разным размером пор), заполненных сегнетоэлектриком − нитратом цезия $CsNO_3$, и изучены их электрофизические свойства. Поверхность пленок контролировалась методом электронной микроскопии. Были измерены температурные зависимости эффективной диэлектрической проницаемости ε' и коэффициента третьей гармоники для нанокомпозитов. Температура фазовых переходов определялась по максимальному значению производной $d\varepsilon'/dT$. Обнаружено, что уменьшение размера пор ведет к снижению температуры Кюри (более, чем на 30 K) и размытию фазового перехода, что связано с влиянием собственных размерных эффектов.

Introduction

Composite materials based on porous nanoscale matrices, such as opal, porous glass, metal oxide films, etc., filled with ferroelectrics, are of interest for practical application in diverse nano-electronics devices [1−3]. The properties of the particles of materials embedded in the matrices are crucial due to a pronounced size effect, as well as the interaction of such inclusions with the walls of the matrix pores; these particles generally have different properties than bulk ferroelectrics. Analysis of experimental data indicates that the size effects are particularly noticeable near structural ferroelectric phase transitions for nanocomposites synthesized by embedding ferroelectrics into nanoporous matrices.

Polar nanoscale structures obtained by introducing ferroelectric particles into the pores of the Al_2O_3 oxide film were considered in [4−11]. It was reported in [4, 5] that stabilization of the ferroelectric phase was detected in a nanoscale composite of Rochelle salt $KNaC_4H_4O_6 \cdot 4H_2O$ embedded in a porous Al_2O_3 film. The ferroelectric phase persists in the composite up to the decomposition temperature of the Rochelle salt (328 K), which in turn is higher than the Curie temperature (about 30 degrees) for the phase transition of the Rochelle salt (297 K). It was discovered in [6] that an increase in the ferroelectric phase is observed for a Rochelle salt composite in a porous Al_2O_3 matrix, due to a simultaneous decrease in the Curie temperature for the first phase transition (255 K), accompanied by an increase in the Curie temperature of the second phase transition (297 K). Shifts in the phase transition temperature were observed in the porous matrices for KNO_3 [8], TGS [4], $SC(NH_2)_2$ [7], $NaNO_2$ [9], KIO_3 [10], $C_6H_{16}NBr$ [11] and a number of other ferroelectric nanocomposites.

Cesium nitrate $CsNO_3$ has ferroelectric properties with a Curie temperature $T_C = 425$ K. Spontaneous polarization of cesium nitrate is small ranging to, according to different data, from 2 $\mu C/cm^2$ [12] to 3.23 $\mu C/cm^2$ [13]. Several studies considered the ferroelectric properties of composite structures based on cesium nitrate [14,15]. In particular, a cesium nitrate nanocomposite, a porous glass, was obtained and studied in [15]. Surface mechanical stresses for cesium nitrate particles embedded in glass pores, arising in the nanocomposite from the matrix led to an increase in the Curie temperature of the composite by 3 K. Moreover, the study discovered that the temperature hysteresis of the phase transition expanded by 9 K in this nanocomposite.

This paper reports on the study of the third harmonic coefficient and permittivity of nanocomposites obtained by embedding cesium nitrate $CsNO_3$ particles into nanoporous Al_2O_3 films with pore sizes of 300 and 240 nm.

Samples and experimental procedure

Cesium nitrate has a trigonal lattice structure with the parameters $a = 10.950$ E and $c = 7.716$ E at room temperature [12]. At $T = 427$ K, cesium nitrate transforms into the cubic phase with the lattice parameter $a = 8.980$ E. Notably, unlike potassium nitrate, the temperature history does not affect the nature of the structural phase transition in cesium nitrate.

Nanocomposites were obtained using chemically pure cesium nitrate and nanoporous aluminum oxide films (manufactured by TopMembranes Technology, China). The size of the cells was 450 nm, the thickness of the films was 50 μm. Two types of films with different pore diameters were used in the experiment: 300 and 240 nm. Fig. 1 shows electronic micrographs of the surfaces of the studied Al_2O_3 films.
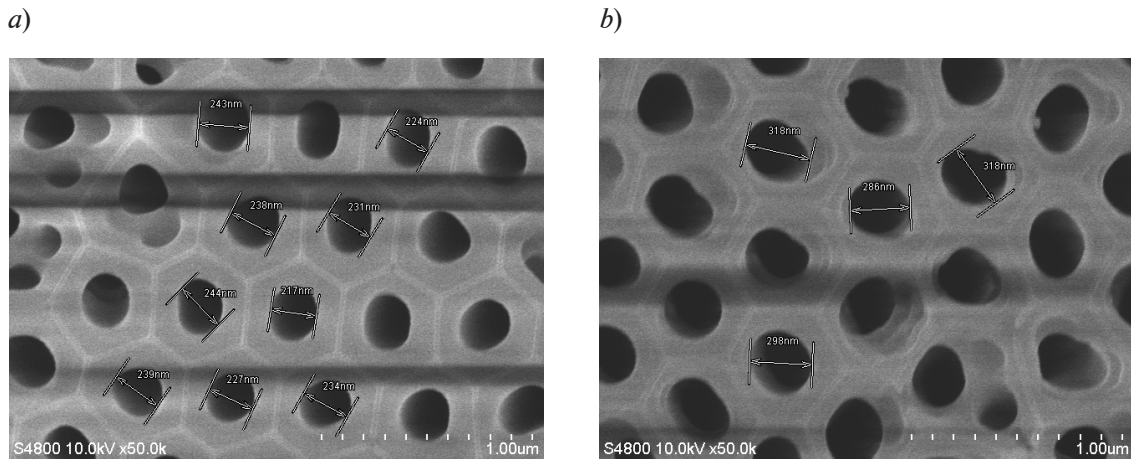
a) *b)*

Fig. 1. SEM images of Al_2O_3 films with pore sizes of 330 nm (*a*) and 240 nm (*b*)

Cesium nitrate was introduced into the pores from a saturated solution of $CsNO_3$ at a temperature of 343−353 K. The solubility of cesium nitrate is significantly lower than that of other nitrates, so the pore filling degrees after 5 cycles of embedding and drying were about 15% and 12%, respectively, for films with pore sizes of 300 and 240 nm. Cylindrical samples of polycrystalline cesium nitrate were used as reference (their diameter and thickness were 10.0 and 1.5 mm, respectively); the samples were obtained by pressing at $8 \cdot 10^3$ kg/cm^2.

An E7-25 digital LCR meter was used to measure the effective permittivity. Methods of nonlinear dielectric spectroscopy were used to detect the polar phase in cesium nitrate. A harmonic signal with a frequency of 2 kHz was applied to the sample, and multi-frequency signals were monitored and recorded on a computer. The presence of a polar phase can be determined by the amplitude and temperature course of the latter signals. The electric field strength of the main signal was approximately 10 V/mm for bulk samples and about 10^4 V/mm for films.

The third harmonic coefficient ($\gamma_{3\omega} = U_{3\omega}/U_{\omega}$) was taken for further analysis, which is the most sensitive to the appearance of a ferroelectric state. The technique for measuring nonlinear dielectric properties is described in detail in [15, 16].

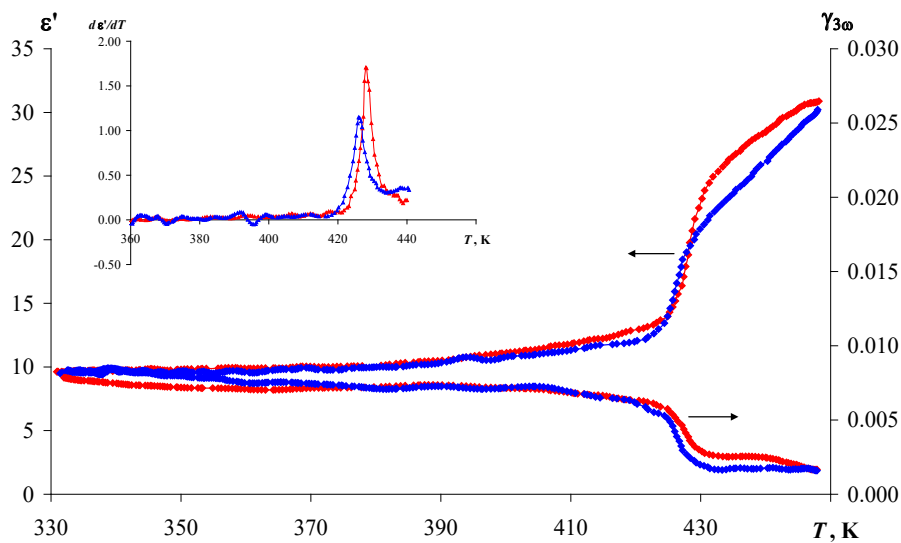
Fig. 2. Temperature dependences of permittivity and third harmonic coefficient
for bulk $CsNO_3$ sample under heating and cooling (red and blue symbols, respectively)
The inset shows the temperature dependences for the variation rate of permittivity under the given conditions

Experimental results and discussion

The graphs in Figs. 2 and 3 represent the temperature dependences of permittivity and the third harmonic coefficient for bulk cesium nitrate and a nanocomposite sample based on a porous oxide film with embedded cesium nitrate with a pore size of 300 nm. The temperature of the phase transitions determined from the maximum value of the derivative $d\varepsilon'/dT$ is 428 K under heating and 426 K under cooling. The third harmonic coefficient exhibits anomalies at the same temperatures, evidencing that the $CsNO_3$ sample makes a transition from the ferroelectric to the paraelectric phase.
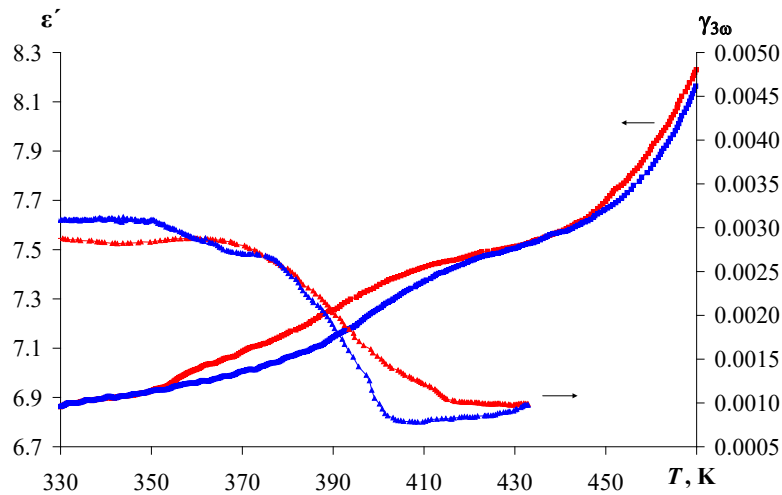

Fig. 3. Temperature dependences of permittivity and the third harmonic coefficient for $CsNO_3/Al_2O_3$ nanocomposite sample with nanoporous film pore size of 300 nm under heating and cooling (red and blue symbols, respectively)

As follows from the graphs in Fig. 3 that the phase transition is significantly smeared for the nanocomposite sample. Despite this, the anomalies on the $\gamma_{3\omega}(T)$ dependence can be used to estimate the temperatures at which spontaneous polarization disappears and appears in cesium nitrate. These temperatures are 416 K under and 405 K under cooling for a film with 300 nm pores. Thus, an increase in the temperature hysteresis of the phase transition from 2 to 11 K is observed.

The third harmonic signal of the $CsNO_3/Al_2O_3$ nanocomposite with a film pore size of 240 nm was at the noise level due to a lower proportion of cesium nitrate. The phase transition was even more smeared, but the transition temperature, determined by the maximum of the derivative $d\varepsilon'/dT$, shifted towards the low-temperature region (Fig. 4). As can be seen in the graphs, the phase transition temperature for a film with a pore size of 240 nm is about (393 ± 1) K under heating and about (387 ± 1) K under cooling.

The smearing and shift in the phase transition temperature towards lower temperatures was previously detected in $Ba_xSr_{1-x}TiO_3$ thin films, which the authors explained by the presence of non-switchable dielectric "dead layers" in the films [17, 18] caused by pinning of the domain walls, i.e., shielding of the internal field with a depleted layer [19−23]. A decrease in the Curie temperature and a smearing in the phase transition were also observed for DTGS in Al_2O_3 films with pores of 300 and 100 nm [24], where this was attributed to intrinsic size effects. A similar situation likely happens for the $CsNO_3/Al_2O_3$ composite (300 and 240 nm).

The decrease in the phase transition temperature in $CsNO_3$ embedded in Al_2O_3 film corresponds to the predictions made by the theoretical Landau and Ising models [25−27]. These models adopt the concept of correlation volume determining the number of ordered dipoles necessary for inducing ferroelectricity. Strong interactions along the polar axis and less strong ones perpendicular to it lead to anisotropy of the correlation volume.

A decrease in the phase transition temperature with a decrease in particle sizes was predicted in earlier studies [25−27]. These assumptions were derived from the theoretical Landau and Ising models based on the concept of correlation volume, determining the number of ordered dipoles, which produces a ferroelectric state.
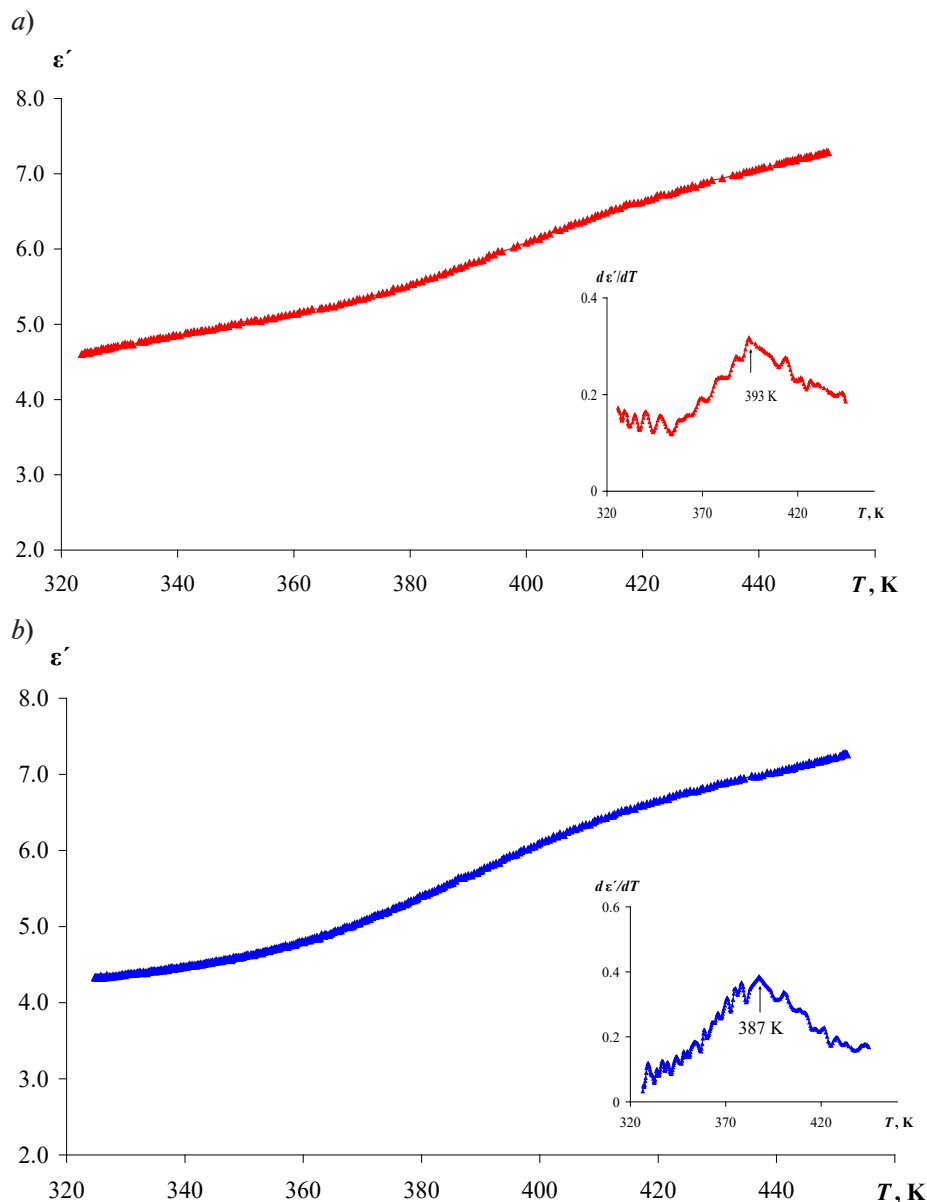
a)

b)

Fig. 4. Temperature dependences of permittivity for $CsNO_3/Al_2O_3$ sample
with the film pore size of 240 nm under heating (*a*) and under cooling (*b*).
The corresponding temperature dependences $d\varepsilon'/dT$ are shown in the insets

The experimental data we obtained for $CsNO_3$ embedded in Al_2O_3 film confirm that these predictions are correct. A possible interpretation of our results is that anisotropy appears in the correlation volume because strong interactions are directed along the polar axis, and less strong ones are perpendicular to it.

As particle sizes decrease below the critical value, the balance between the long-range and the short-range forces is disrupted and the ferroelectric state is destabilized; a paraelectric phase is consequently formed. These models suggest that the phase transition temperature shifts deep into the ferroelectric phase as the sizes of isolated spherical or cylindrical nanoparticles decrease. The results obtained for isolated small particles of barium titanate can serve as a confirmation for this explanation (see [28] and references therein).

Interactions between polar particles and pore walls, as well as dipole-dipole interactions between particles in adjacent pores can influence the temperature of the ferroelectric phase transition, along with its intrinsic size effect [28−33]. The directions of the dipole moments of particles located in adjacent pores of the matrix can contribute to both an increase and a decrease in the Curie temperature.

The influence of mechanical stresses on the ferroelectric properties of nanoparticles was considered in [29−31]. It was established that the interaction of the embedded substance with the matrix walls, geneally leads to an increase in the temperature of the ferroelectric phase transition. For this reason, it can be assumed that the role of mechanical stresses in the $CsNO_3/Al_2O_3$ nanocomposite is minimal as the pores are only partially filled (by no more than $12−15\%$). On the other hand, the low level of spontaneous polarization and the considerable distances between the pores weaken the influence of dipole-dipole interaction. Thus, we can exclude the effect of mechanical stresses and the role of dipole-dipole interaction on the variation in the phase transition temperature of the $CsNO_3/Al_2O_3$ composite. However, if we assume that the particles of the embedded substance exist in the pores as a system of small crystallites whose dimensions are significantly smaller than the diameter of the pores, then we can hypothesize that the decrease in the phase transition temperature in $CsNO_3/Al_2O_3$ is due to the intrinsic size effect.

Ferroelectric nanoparticles embedded into matrix materials are characterized by a significant smearing of the phase transition maximum, as discussed in a number of theoretical studies. This phenomenon can be attributed to a wide range of cause related to non-uniform distribution of elastic strains and internal electric fields. Similar processes are typical for disordered ferroelectric structures and solid solutions. A gradual transition from the disordered to the ordered phase is observed in a wide temperature range called the Curie region. This region is characterized by a gradual change in such ferroelectric properties as spontaneous polarization, piezoelectric moduli, anomalous specific heat capacity, and others.

Conclusion

The results of dielectric studies of cesium nitrate particles embedded in nanoporous aluminum oxide films suggest that a decrease in the pore size leads to a decrease in the Curie temperature and a smearing of the phase transition, which is most likely due to intrinsic size effects.

REFERENCES

1. **Stadlober B., Zirkl M., Irimia-Vladu M.,** Route towards sustainable smart sensors: ferroelectric polyvinylidene fluoride-based materials and their integration in flexible electronics, Chem. Soc. Rev. 48(6) (2019) 1787−1825.

2. **Jin R. B., Cai N., Huang Y., et al.,** Theoretical investigation of a spectrally pure-state generation from isomorphs of KDP crystal at near-infrared and telecom wavelengths, Phys. Rev. Appl. 11 (3) (2019) 034067.

3. **Kasap S., Capper P.** (Eds.), Springer handbook of electronic and photonic materials, Springler-Verlag US, New York, 2007.

4. **Rogazinskaya O. V., Milovidova S. D., Sidorkin A. S., et al.,** Properties of nanoporous aluminum oxide with with triglycine sulfate and Rochelle salt inclusions, Phys. Solid State. 51 (7) (2009) 1518−1520.

5. **Yadlovker D., Berger S.,** Uniform orientation and size of ferroelectric domains, Phys. Rev. B. 71 (18) (2005) 184112.

6. **Baryshnikov S. V., Stukova E. V., Milinskiy A. Yu., et al.,** Ferroelectricity in Rochelle salt nanoparticles confined to porous alumina, Ferroelectrics. 396 (1) (2010) 3−9.

7. **Milinskii A. Y., Baryshnikov S. V., Antonov A. A.,** Phase transitions of $SC(NH_2)_2$ferroelectricsin Al_2O_3-based nanoporous matrices, Phys. Solid State. 59 (9) (2017) 1783−1788.

8. **Rogazinskaya O. V., Sidorkin A. S., Popravko N. G., et al.,** Dielectric and repolarization properties of nanocomposites based on porous matrix with sodium nitrite, Ferroelectrics. 469 (1) (2014) 138−143.

9. **Alekseeva O. A., Naberezhnov A. A., Stukova E. V., et al.,** Temperature range broadening of the ferroelectric phase in KNO_3 nanoparticles embedded in the pores of the nanoporous Al_2O_3 matrix, Ferroelectrics. 574 (1) (2921) 8−15.

10. **Milinskii A. Y., Baryshnikov S. V.,** Phase transitions of KIO_3ferroelectrics in Al_2O_3-based nanoporous matrices,Phys. Solid State. 60 (3) (2018) 549−552.

11. **Milinskiy A. Yu., Baryshnikov S. V., Egorova I. V., et al.,** Dielectric properties of an organic ferroelectrics of bromide diisopropylammonium embedded into the pores of nanosized Al_2O_3 films, J. Phys. Condens. 31 (48) (2019) 485704.

12. **Lucas B. W.,** The structure (neutron) of phase II cesium nitrate at 298 K, $CsNO_3$, Acta Crystallogr. C. Struct. Chem. C39(12) (1983)1591−1594.

13. **Nautiyal A., Sekhar K. C., Pathak N. P., Nath R.,** Study of ferroelectric properties of spray pyrolysis deposited cesium nitrate films, Thin Solid Films. 518 (24, Suppl,) (2010) e143−e145.

14. **Rao M. V. M., Reddy S. N., Chary A. S.,** Enhancement of DC ionic conductivity in dispersed solid electrolyte system $CsNO_3$: γ-Al_2O_3, Phys. B Condens. 389(2) (2007) 292−295.

15. **Milinskiy A. Y., Baryshnikov S. V., Chernechkin I. A.,** Dielectric and thermal properties of cesium nitrate−porous glass nanocomposite, Russ. Phys. J. 65 (9) (2023) 1431−1435.

16. **Ikeda S., Kominami H., Koyama K., Wada Y. J.,** Nonlinear dielectric constant and ferroelectric-to-paraelectric phase transition in copolymers of vinylidenefluoride and trifluoroethylene, J. Appl. Phys. 62 (8) (1987) 3339−3342.

17. **Vendik O. G., Zubko S. P.,** Ferroelectric phase transition and maximum dielectric permittivity of displacement type ferroelectrics ($Ba_xSr_{1-x}TiO_3$), J. Appl. Phys. 88 (9) (2000) 5343−5350.

18. **Lookman A., Bowman R. M., Gregg J. M., et al.,** Thickness independence of true phase transition temperatures in barium strontium titanate films. J. Appl. Phys. 96 (1) (2004) 555−562.

19. **Larsen P. K., Dormans G. J. M., Taylor D. J., van Yeldhoven P. J.,** Ferroelectric properties and fatigue of $PbZr_{0.51}Ti_{0.49}O_3$ thin films of varying thickness: Blocking layer model, J. Appl. Phys. 76 (4) (1994) 2405−2413.

20. **Miller S. L., Nasbv R. D., Schwank J. R., et al.,** Device modeling of ferroelectric capacitors,J. Appl. Phys. 68 (12) (1990) 6463−6471.

21. **Tagantsev A. K., Landivar M., Colla E., Setter N.,** Identification of passive layer in ferroelectric thin films from their switching parameters, J. Appl. Phys. 78 (4) (1995) 2623−2630.

22. **Lebedev N. I., Sigov A. S.,** Surface inhomogeneties and coercive field of thin ferroelectric film, Integr. Ferroelectr. 4 (1) (1994) 21−24.

23. **Tagantsev A. K.,** Size effects in polarization switching in ferroelectric thin films, Integr. Ferroelectr. 16 (1−4) (1997) 237−244.

24. **Stukova E., Baryshnikov S., Baryshnikova T., Solnyshkin A.,** Linear and non-linear dielectric properties of DTGS in porous Al_2O_3 films, Ferroelectrics. 543 (1) (2019) 184−190.

25. **Zhong W. L., Wang Y. G., Zhang P. L., Qu B. D.,** Phenomenological study of the size effect on phase transitions in ferroelectric particles, Phys. Rev. B. 50 (2) (1994) 698−703.

26. **Wang Y. G., Zhong W. L., Zhang P. L.,** Size driven phase transition in ferroelectric particles, Solid State Commun. 90 (5) (1994) 329−332.

27. **Wang C. L., Xin Y., Wang X. S., Zhong W. L.,** Size effects of ferroelectric particles described by the transverse Ising model,Phys. Rev. B. 62 (17) (2000) 11423−11427.

28. **Sedykh P., Michel D.,** Ferroelectric phase transition in barium titanate nanoparticles, Phys. Rev. B. 79 (13) (2009) 134119.

29. **Shchukin V. A., Bimberg D.,** Spontaneous ordering of nanostructures on crystal surfaces, Rev. Modern Phys. 71 (4) (1999) 1125−1171.

30. **Morozovska A. N., Glinchuk M. D., Eliseev E. A.,** Phase transitions induced by confinement of ferroic nanoparticles, Phys. Rev. B. 76 (1) (2007) 014102.

31. **Morozovska A. N., Eliseev E. A., Glinchuk M. D.,** Size effects and depolarization field influence on the phase diagrams of cylindrical ferroelectric nanoparticles, Phys. B. Cond. 387 (1−2) (2007) 358−366.

32. **Charnaya E. V., Pirozerskii A. L., Tien C., Lee M. K.,** Ferroelectricity in an array of electrically coupled confined small particles, Ferroelectrics. 350 (1) (2007) 75−80.

СПИСОК ЛИТЕРАТУРЫ

1. **Stadlober B., Zirkl M., Irimia-Vladu M.** Route towards sustainable smart sensors: ferroelectric polyvinylidene fluoride-based materials and their integration in flexible electronics // Chemical Society Reviews. 2019. Vol. 48. No. 6.Pp. 1787−1825.

2. **Jin R. B., Cai N., Huang Y., Hao X.-Y., Wang S., Li F., Song H.-Zh., Zhou Q., Shimizu R.** Theoretical investigation of a spectrally pure-state generation from isomorphs of KDP crystal at near-infrared and telecom wavelengths // Physical Review Applied. 2019. Vol. 11. No. 3. P. 034067.

3. **Kasap S., Capper P.** (Eds.) Springer handbook of electronic and photonic materials. New York: Springler-Verlag, US, 2007. 1407 p.

4. **Рогазинская О. В., Миловидова С. Д., Сидоркин А. С., Чернышев В. В., Бабичева Н. Г.** Свойства нанопористого оксида алюминия с включениями триглицинсульфата и сегнетовой соли // Физика твердого тела. 2009. Т. 7 № .51. С. 1432−1430.

5. **Yadlovker D., Berger S.** Uniform orientation and size of ferroelectric domains // Physical Review B. 2005. Vol. 71. No. 18. P. 184112.

6. **Baryshnikov S. V., Stukova E. V., Milinskiy A. Yu., Charnaya E. V., Tien C.** Ferroelectricity in Rochelle salt nanoparticles confined to porous alumina // Ferroelectrics. 2010. Vol. 396. No. 1. Pp. 3−9.

7. **Милинский А. Ю., Барышников С. В., Антонов А. А.** Исследование фазовых переходов сегнетоэлектрика $SC(NH_2)_2$ в нанопористых матрицах на основе Al_2O_3 // Физика твердого тела. 2017. Т. 59. № 9. С. 1759−1764.

8. **Rogazinskaya O. V., Sidorkin A. S., Popravko N. G., Milovidova S. D., Naberezhnov A. A., Grokhotova E. V.** Dielectric and repolarization properties of nanocomposites based on porous matrix with sodium nitrite // Ferroelectrics. 2014. Vol. 469. No. 1. Pp. 138−143.

9. **Alekseeva O. A., Naberezhnov A. A., Stukova E. V., Baryshnikov S. V., Franz A.** Temperature range broadening of the ferroelectric phase in KNO_3 nanoparticles embedded in the pores of the nanoporous Al_2O_3 matrix // Ferroelectrics. 2021. Vol. 574. No. 1. Pp. 8−15.

10. Милинский **А. Ю.**, Барышников С. В. Исследование фазовых переходов сегнетоэлектрика KIO_3 в нанопористых матрицах на основе пленок Al_2O_3 // Физика твердого тела. 2018. Т. 60. № 3. С. 543−546.

11. **Milinskiy A. Yu., Baryshnikov S. V., Egorova I. V., Charnaya E. V., Nguyen H. T.** Dielectric properties of an organic ferroelectrics of bromide diisopropylammonium embedded into the pores of nanosized Al_2O_3 films // Journal of Physics: Condensed Matter. 2019. Vol. 31. No. 48. P. 485704.

12. **Lucas B. W.** The structure (neutron) of phase II cesium nitrate at 298 K, $CsNO_3$ // Acta Crystallographica. Section C: Structural Chemistry. 1983. Vol. C39. Part 12. Pp. 1591−1594.

13. **Nautiyal A., Sekhar K. C., Pathak N. P., Nath R.** Study of ferroelectric properties of spray pyrolysis deposited cesium nitrate films // Thin Solid Films. 2010. Vol. 518. No. 24, Supplement. Pp. e143−e145.

14. **Rao M. V. M., Reddy S. N., Chary A. S.** Enhancement of DC ionic conductivity in dispersed solid electrolyte system $CsNO_3{:}\gamma{-}Al_2O_3$ // Physica B: Condensed Matter. 2007. Vol. 389. No. 2. Pp. 292−295.

15. Милинский **А. Ю.**, Барышников С. В., Чернечкин **И.** А. Диэлектрические и тепловые свойства нанокомпозита нитрат цезия − пористое стекло // Известия высших учебных заведений. Физика. 2022. Т. 65. № 9. С. 15−19.

16. **Ikeda S., Kominami H., Koyama K., Wada Y. J.** Nonlinear dielectric constant and ferroelectric-to-paraelectric phase transition in copolymers of vinylidenefluoride and trifluoroethylene // Journal of Applied Physics. 1987. Vol. 62. No. 8. Pp. 3339−3342.

17. **Vendik** O. **G., Zubko S. P.** Ferroelectric phase transition and maximum dielectric permittivity of displacement type ferroelectrics ($Ba_xSr_{1-x}TiO_3$) // Journal of Applied Physics. 2000. Vol. 88. No. 9. Pp. 5343−5350.

18. **Lookman A., Bowman R. M., Gregg J. M., Kut J., Rios S., Dawber M., Ruediger A., Scott J. F.** Thickness independence of true phase transition temperatures in barium strontium titanate films // Journal of Applied Physics. 2004. Vol. 96. No. 1. Pp. 555−562.

19. **Larsen P. K., Dormans G. J. M., Taylor D. J., van Yeldhoven P. J.** Ferroelectric properties and fatigue of $PbZr_{0.51}Ti_{0.49}O_3$ thin films of varying thickness: Blocking layer model // Journal of Applied Physics. 1994. Vol. 76. No. 4. Pp. 2405−2413.

20. **Miller S. L., Nasbv R. D., Schwank J. R., Rodgers M. S., Dressendorfer P. V.** Device modeling of ferroelectric capacitors // Journal of Applied Physics. 1990. Vol. 68. No. 12. Pp. 6463−6471.

21. **Tagantsev A. K., Landivar M., Colla E., Setter N.** Identification of passive layer in ferroelectric thin films from their switching parameters // Journal of Applied Physics. 1995. Vol. 78. No. 4. Pp. 2623−2630.

22. **Lebedev N. I., Sigov A. S.** Surface inhomogeneties and coercive field of thin ferroelectric film // Integrated Ferroelectrics. 1994. Vol. 4. No. 1. Pp. 21−24.

23. **Tagantsev A. K.** Size effects in polarization switching in ferroelectric thin films // Integrated Ferroelectrics. 1997. Vol. 16. No 1−4. Pp. 237−244.

24. **Stukova E., Baryshnikov S., Baryshnikova T., Solnyshkin A.** Linear and non-linear dielectric properties of DTGS in porous Al_2O_3 films // Ferroelectrics. 2019. Vol. 543. No. 1. Pp. 184−190.

25. **Zhong W. L., Wang Y. G., Zhang P. L., Qu B. D.** Phenomenological study of the size effect on phase transitions in ferroelectric particles // Physical Review B. 1994. Vol. 50. No. 2. Pp. 698−703.

26. **Wang Y. G., Zhong W. L., Zhang P. L.** Size driven phase transition in ferroelectric particles // Solid State Communications. 1994. Vol. 90. No 5. Pp. 329−332.

27. **Wang C. L., Xin Y., Wang X. S., Zhong W. L.** Size effects of ferroelectric particles described by the transverse Ising model // Physical Review B. 2000. Vol. 62. No. 17. Pp. 11423−11427.

28. **Sedykh P., Michel D.** Ferroelectric phase transition in barium titanate nanoparticles // Physical Review B. 2009. Vol. 79. No. 13. P. 134119.

29. **Shchukin V. A., Bimberg D.** Spontaneous ordering of nanostructures on crystal surfaces // Review of Modern Physics. 1999. Vol. 71. No. 4. Pp. 1125−1171.

30. **Morozovska A. N., Glinchuk M. D., Eliseev E. A.** Phase transitions induced by confinement of ferroic nanoparticles // Physical. Review. B. 2007. Vol. 76. No. 1. P. 014102.

31. **Morozovska A. N., Eliseev E. A., Glinchuk M. D.** Size effects and depolarization field influence on the phase diagrams of cylindrical ferroelectric nanoparticles // Physica B: Condensed Matter. 2007. Vol. 387. No. 1−2. Pp. 358−366.

32. **Charnaya E. V., Pirozerskii A. L., Tien C., Lee M. K.** Ferroelectricity in an array of electrically coupled confined small particles // Ferroelectrics. 2007. Vol. 350. No. 1. Pp. 75−80.

THE AUTHORS

PAVLOV Aleksei V.
Amur State University
21 Ignatievskoe Ave., Blagoveshchensk, 675027, Russia
katal75@yandex.ru
ORCID: 0000-0002-7287-2006

STUKOVA Elena V.
Amur State University
21 Ignatievskoe Ave., Blagoveshchensk, 675027, Russia
lenast@bk.ru
ORCID: 0000-0002-7981-7456

BARYSHNIKOV Sergey V.
Blagoveschensk State Pedagogical University
104 Lenin St., Blagoveshchensk, 675000, Russia
svbar2003@list.ru
ORCID: 0000-0002-3362-8975

СВЕДЕНИЯ ОБ АВТОРАХ

ПАВЛОВ Алексей Владимирович — *аспирант кафедры физики Амурского государственного университета.*

675027, Россия, Амурская область, г. Благовещенск, Игнатьевское шоссе, 21

katal75@yandex.ru

ORCID:0000-0002-7287-2006

СТУКОВА Елена Владимировна — *доктор физико-математических наук, профессор кафедры физики Амурского государственного университета.*

675027, Россия, Амурская область, г. Благовещенск, Игнатьевское шоссе, 21

lenast@bk.ru

ORCID:0000-0002-7981-7456

БАРЫШНИКОВ Сергей Васильевич — *доктор физико-математических наук, профессор кафедры физического и математического образования Благовещенского государственного педагогического университета.*

675000, Россия, Амурская область, г. Благовещенск, ул. Ленина, 104

svbar2003@list.ru

ORCID:0000-0002-3362-8975